

Multisensor 3D Posture Determination of a Mobile Robot Using Inertial and Ultrasonic Sensors

CHING-CHIH TSAI, HUNG-HSING LIN and SZU-WEI LAI

Department of Electrical Engineering, National Chung Hsing University, Taichung, Taiwan 40227, Republic of China; e-mail: cctsai@dragon.nchu.edu.tw

(Received: 2 July 2004; in final form: 22 February 2005)

Abstract. This paper presents methodologies and techniques for fusing inertial and ultrasonic sensors to estimate the current posture of a mobile robot navigating over indoor uneven terrain. This new type of pose tracking system is developed by means of fusing an inertial navigation subsystem (INS) and an ultrasonic localization subsystem. Extended Kalman filtering (EKF)-based algorithm for integrating both the subsystems is proposed to obtain reliable attitude and position estimates of the vehicle and to eliminate the accumulation errors caused by wheel slippage and surface roughness. Experimental results are conducted to illustrate feasibility and effectiveness of the proposed system and method.

Key words: extended Kalman filtering (EKF), inertial navigation system, mobile robot, posture determination, ultrasonics.

1. Introduction

Over the decades, mobile robots have already found widespread applications in automated factories, offices, hospitals and warehouses. Mobile robots are also becoming increasingly important in areas where work is hazardous to humans. These areas include mining, explosive and toxic material handling, and nuclear power plant operations. More significant research efforts are underway for using mobile robots to perform more complicated missions in military, space exploration and human service applications. In these applications, the posture determination or localization capability of mobile robots is extremely important for free-ranging path tracking as well as reactive navigation in any given environment (Leonard and Durrant-Whyte, 1992; Maksarov and Durrant-Whyte, 1995; Fujisawa et al., 2001). The posture determination technology for mobile robots means to calculate its current position and orientation with respect to a given inertial reference frame (Borenstein et al., 1996; Drumheller, 1987). For this purpose, many multisensorial 2D dead-reckoning (DR) approaches have been successfully applied to determine the current postures of mobile robots navigating at a flat floor and traveling over short distances (Tsai, 1998). However, the detrimental factors, such as slippage, surface roughness and misalignment of wheels, cause the accumulation errors of these dead-reckoning methods to grow without bounds. Moreover, such methods

cannot be directly applicable to the vehicle traveling over any steep gradient and undulating terrain (Song and Suen, 1996). A 3D dead-reckoning (DR) method has been proposed by Lai (2000) to overcome such shortcomings. However, if the traveling terrain is irregularly uneven, this type of 3D DR approach may quickly fail to keep track of its postures even over short distances (Kim et al., 1995).

The paper aims at developing a new indoor 3D posture determination system of the robot based on both inertial and ultrasonic measurements (Figuroa and Mahajan, 1994). This posture tracking system is expected to be suitable for every mobile vehicle traveling over indoor uneven terrain. This novel system is composed of an inertial navigation subsystem (INS) and an ultrasonic localization subsystem. The proposed inertial navigation system is an alternative sophisticated implementation of internal navigation system, which particularly uses inertial sensors such as gyroscopes, speedometers, and accelerometers to measure the angular velocity, the linear velocity and acceleration with respect to the inertial frame. The gyroscopic angular velocity can be integrated to provide the attitude for the robot, the linear acceleration from accelerometers can be integrated to provide the velocity, and the linear velocity from speedometers can be integrated to provide the distance for the robots. Consequently, the type of inertial navigation system is regarded as a self-contained, nonradiating, high-precision and short time-duration navigation system. This technique is expected to effectively eliminate the errors caused by wheel slippage and surface roughness (Barshan and Durrant-Whyte, 1994; Mae et al., 2001). Like the DR method, the navigation errors in an INS have a tendency to increase with time due to noise input and the drifts of the inertial sensors. The fundamental error sources contained in gyroscope and accelerometer measurements affect the accuracy of an INS over long traveling distances. Fortunately, such errors can be eliminated by using a 3D ultrasonic localization system proposed by Tsai et al. (2003). The position calibration capability of the 3D ultrasonic localization system has been proven useful in providing the robot's posture in a small limited area quickly, accurately and inexpensively. Thus, the INS can be adopted for supplying the information of vehicle maneuvering in the absence of ultrasonic signals, and the 3D ultrasonic localization system mounted at many specified locations is used to compensate for the long-distance accumulated errors when the vehicles are passing through the designated regions (Figuroa and Mahajan, 1994; Sabatini, 1995). The INS together with the ultrasonic system is capable of building an alternative integrated navigation system for three-dimensional vehicle navigation over indoor uneven terrain.

In this paper, an integration method, previously appeared in (Maybeck, 1979; Kim et al., 1995; Wang et al., 2003), will be applied to the new integrated system. This method is expected to address the problem of the 3D posture determination for a mobile robot in the absence of wheel encoder or odometer information, assuming that the robot has pneumatic tires without suspension and runs over a road surface at speeds below 1 m/sec in any given indoor uneven terrain. To make best use of low-cost inertial sensing systems, we use two types of Kalman filters; one is for the

INS, and the other is for the INS with ultrasonic localization system (Vaganay et al., 1993; Triggs, 1994; Foxlin, 2002). This type of hardware implementation for the integrated system reduces the computing loads and increases the positioning accuracy (Sorenson, 1990; Maybeck, 1979). Figure 1 shows a block diagram of the integrated system.

The remainder of the paper is organized as follows. Section 2 briefly describes the posture determination system. The multisensorial INS subsystem is developed in Section 3. Section 4 explores how to use the Extended Kalman filtering to fuse the INS and ultrasonic temporal data. Two experiments are described which have been performed in Section 5 to verify the accuracy and performance of the proposed method. Section 6 concludes the paper.

2. System Configuration

Figure 2 displays the physical configuration of the multisensorial INS subsystem mounted on a laboratory-based autonomous mobile robot, having two independently driving front wheels and two freely rotating back wheels. The multisensorial INS subsystem is constructed by using three gyroscopes, one speedometer, and one triaxial accelerometer and two high-resolution optical incremental shaft encoders mounted on the front driving wheels. Two optical incremental encoders are employed as a speedometer for computing the velocity of the robot. The digital fluxgate compass provides a measure of absolute robot heading by sensing and processing the averaged strength of the earth's magnetic field. In contrast to the compass, the rategyro periodically produces nonjammable, relative robot heading measurements by integrating its instantaneous angular velocity over a period. The notebook computer system with an analog and digital signal interfacing board is responsible for performing the sensing procedures, executing multisensorial INS and sensor fusion algorithms and storing the results.

Figure 3 depicts the physical configuration of the novel 3D ultrasonic location system which consists of one RF controlled ultrasonic transmitter mounted on the known location fixed to an inertial frame of reference, and four ultrasonic receivers and one RF controlled switch placed on the mobile robot. For the system, an ultrasonic transmitter T_5 is mounted at a known location (x_5, y_5, z_5) , and four ultrasonic receivers having the right triangle structure are installed on the mobile robot. The receivers' locations are denoted by $R_1 = (x_1, y_1, z_1)$, $R_2 = (x_2, y_2, z_2)$, $R_3 = (x_3, y_3, z_3)$ and $R_4 = (x_4, y_4, z_4)$, respectively. Moreover, let the center of the receiver module be represented by (x, y, z) , and then the positions of receivers R_1 , R_2 , R_3 and R_4 are expressed by

$$\begin{aligned} x_1 &= x - d \cos(60^\circ - \theta) = x - 0.5 \cdot d \cos \theta - \frac{\sqrt{3}}{2} d \sin \theta, \\ y_1 &= y + d \sin(60^\circ - \theta) = y + \frac{\sqrt{3}}{2} \cos \theta - 0.5 \cdot d \sin \theta, \\ z_1 &= z, \end{aligned}$$

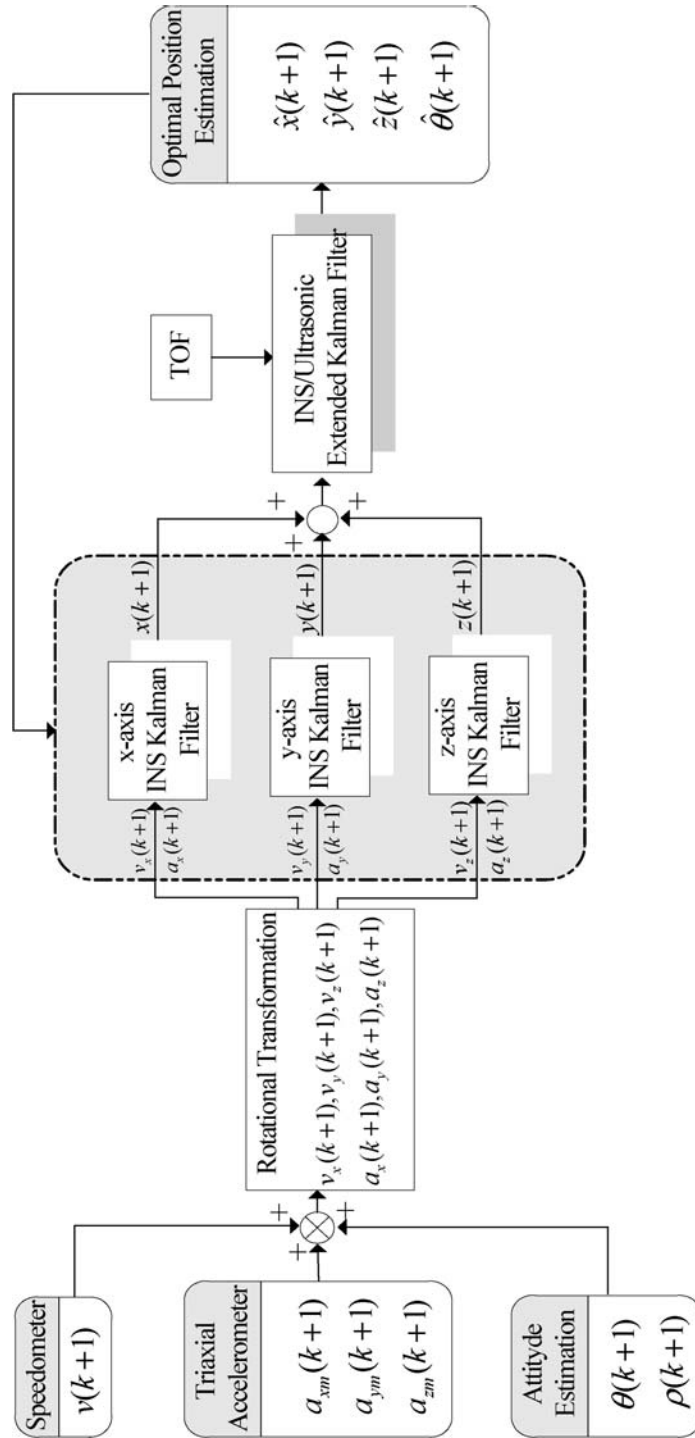


Figure 1. Block diagram of the INS/ultrasonic location system.

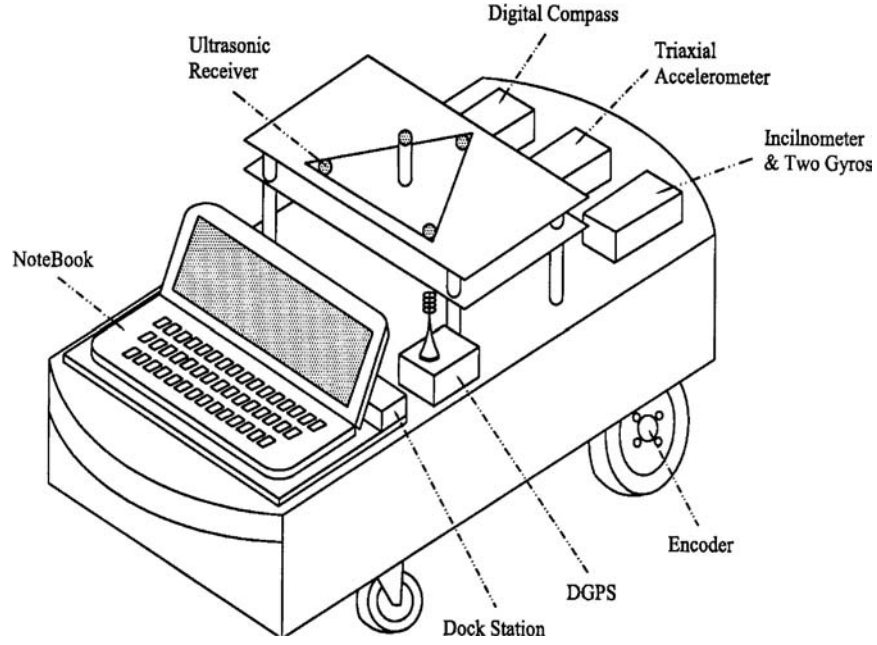


Figure 2. Physical configuration of a multisensorial posture determination system mounted on a laboratory-based autonomous wheeled mobile robot.

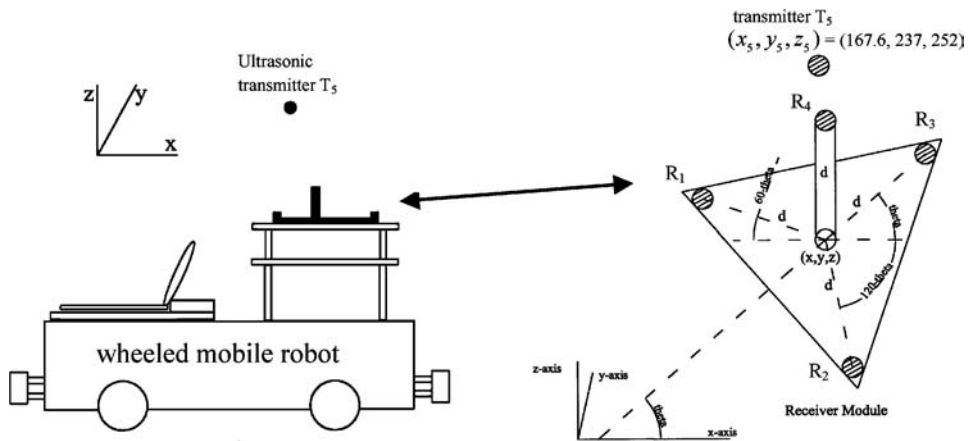


Figure 3. Physical configuration of the proposed 3D Ultrasonic location system.

$$\begin{aligned}
 x_2 &= x + d \cos(120^\circ - \theta) = x - 0.5 \cdot d \cos \theta + \frac{\sqrt{3}}{2} d \sin \theta, \\
 y_2 &= y - d \sin(120^\circ - \theta) = y - \frac{\sqrt{3}}{2} \cos \theta - 0.5 \cdot d \sin \theta, \\
 z_2 &= z, \\
 x_3 &= x + d \cos \theta, & y_3 &= y + d \sin \theta, & z_3 &= z; \\
 x_4 &= x, & y_4 &= y, & z_4 &= z + d,
 \end{aligned}$$

where d represents the distance from the middle module to each receiver and θ is the vehicle heading. The scenario for measuring the TOF data between the ultrasonic transmitter/receiver modules is stated as follows. First, the ultrasonic transmitter immediately sends out a modulated signal after receiving a starting signal via the RF switch controlled by the computer. Second, each 16-bit counter with 2 MHz counting rate accumulates the TOF data until the corresponding receiver confirms that the ultrasonic modulated signal has been received. The method used for the TOF measurements is based on a simple threshold detection with a time varying gain-scheduled amplifier and a capacitive charge-up circuit. Finally, the computer reads all the TOF data via designed digital interfacing circuits and then starts to execute the robot location determination algorithm. The whole measurement process is periodically repeated and the sampling rate depends upon the vehicle's linear speed. Worthy of mention is that the system may fail to receive TOF data when the robot moves out the effective coverage of the ultrasonic wave propagation.

The attitude estimate of the vehicle relies on the measurements from the digital compass, the liquid-filled inclinometer and the two gyros. When the vehicle is in motion, the estimation of pitch $\rho(t)$ is by cascading the tilt sensor, the rate gyro and a Kalman filter. In the meantime, the determination of yaw angle $\theta(t)$ is achieved via a combination of the compass, the rate gyro and a Kalman filter.

3. Multisensorial INS System

Inertial navigation systems are self-contained, nonradiating, nonjammable, dead-reckoning navigation systems that provide continuous position and orientation information through direct measurements. Unlike commercially airborne INS, the type of the proposed INS is integrated with the absolute location-sensing devices to provide useful information about the vehicle position, the gyroscopes to provide angular rate information, and the accelerometers to provide acceleration rate information. The rate information together with the tilt sensors, the compass and the speedometer gives more accurate absolute measurements of attitude and position of the vehicle.

3.1. ROTATIONAL COORDINATE TRANSFORMATION

This subsection considers a three-dimensional coordinate transformation in which the measurements are represented in the world frame $X-Y-Z$. Since the triaxial accelerometer measurement data represents the acceleration of the robot in the mobile robot frame $X_m-Y_m-Z_m$, a rotational transformation through Euler angles, yaw and pitch angles, around X , Y and Z axes must be utilized to transform the readings in the mobile moving frame $X_m-Y_m-Z_m$ into those in the world frame. Figure 4 illustrates this relationship between the mobile moving frame $X_m-Y_m-Z_m$ and the world frame $X-Y-Z$.

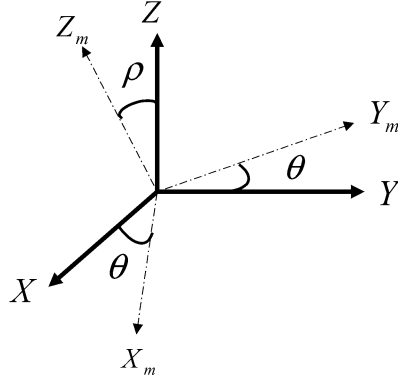


Figure 4. Relationship between the moving frame X_m - Y_m - Z_m and the world frame X - Y - Z .

3.2. ACCELEROMETER TRANSFORMATION

The accelerometer mounted on the laboratory-based autonomous mobile robot is particularly used to measure the three-dimensional local gravitational acceleration $a_{x_m}(k)$, $a_{y_m}(k)$, $a_{z_m}(k)$ in the mobile robot frame. Hence the rotational transformation equation (1) is used to convert $a_{x_m}(k)$, $a_{y_m}(k)$, $a_{z_m}(k)$, shown in Figure 5, into $a_x(k)$, $a_y(k)$, $a_z(k)$ in the world frame.

$$\begin{aligned} a_x &= a_{x_m} \cos \theta \cdot \cos \rho - a_{y_m} \sin \theta \cdot \cos \rho - a_{z_m} \sin \theta \cdot \sin \rho, \\ a_y &= a_{x_m} \sin \theta \cdot \cos \rho + a_{y_m} \cos \theta \cdot \cos \rho - a_{z_m} \cos \theta \cdot \sin \rho, \\ a_z &= a_{x_m} \sin \rho + a_{y_m} \sin \theta + a_{z_m} \cos \rho. \end{aligned} \quad (1)$$

Note that $a_x(k)$, $a_y(k)$ and $a_z(k)$ represent the three-dimensional accelerations of the robot in the world frame, and they are related to the measured accelerations by a rotational transformation through the Euler angles θ , ρ around x , y and z axes, respectively.

The velocities $v_x(k)$, $v_y(k)$, $v_z(k)$ in the world frame X - Y - Z are then approximated by

$$\begin{aligned} v_x(k+1) &= v_x(k) + \Delta t \cdot a_x(k), \\ v_y(k+1) &= v_y(k) + \Delta t \cdot a_y(k), \\ v_z(k+1) &= v_z(k) + \Delta t \cdot a_z(k). \end{aligned} \quad (2)$$

3.3. VELOCITY TRANSFORMATION

The linear velocity of the vehicle is expressed using

$$v(t) = \frac{R}{2r}(\omega_R(t) + \omega_L(t)), \quad (3)$$

where $r = 27$ denotes the gear ratio, $R = 10.75$ cm represents the radius of the drive wheels, $\omega_R(t)$ and $\omega_L(t)$ are the angular velocity outputs of the right and left motors, respectively.

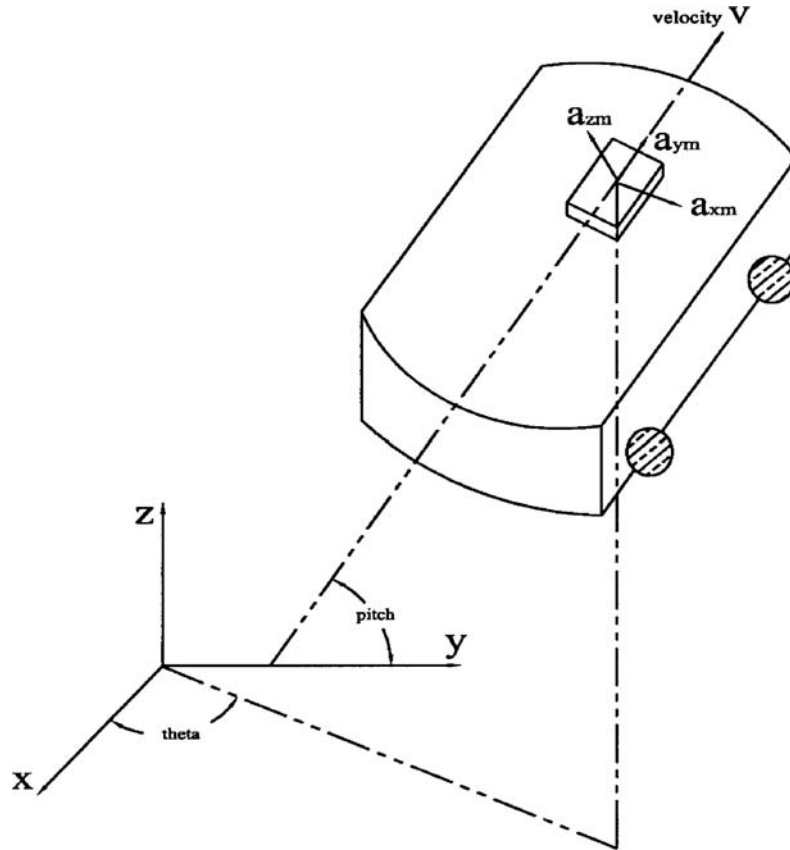


Figure 5. Velocity and acceleration measurements with respect to the world frame.

This study assumes the sampling interval of vehicle sensors (triaxial accelerometer, speedometer) short enough in comparison with the changing rates of the vehicle's moving velocity and acceleration. By utilizing a rotational transformation between the Cartesian frame and the spherical frame, we can obtain the three axis velocities of the robot.

$$\begin{aligned}
 v_x(k) &= v(k) \cos \rho(k) \cos \theta(k), \\
 v_y(k) &= v(k) \cos \rho(k) \sin \theta(k), \\
 v_z(k) &= v(k) \sin \rho(k).
 \end{aligned}
 \tag{4}$$

Hence, the position in the world frame X - Y - Z is then calculated by

$$\begin{aligned}
 x(k+1) &= x(k) + \Delta t \cdot v_x(k), \\
 y(k+1) &= y(k) + \Delta t \cdot v_y(k), \\
 z(k+1) &= z(k) + \Delta t \cdot v_z(k).
 \end{aligned}
 \tag{5}$$

3.4. LOCALIZATION ESTIMATION

A fundamental capability of an autonomous mobile robot is its ability to localize itself with respect to its reference frame. To do so, the inertial navigation system (INS) of the laboratory-based autonomous mobile robot consists of a sensor module, which includes speedometer, triaxial accelerometer and attitude estimation system. Based on these signal measurements, the three-dimensional velocity and position vectors are then computed. Since there is no device measuring the absolute position of the robot, the position can only be estimated through the integration of the accelerometer signals and speedometer signals. The speedometer is mainly used for the calculation of the traveled distance and the accelerometer is adopted to obtain the position estimate.

For this study, the Kalman filter is used as a navigation sensor fusion processor. This type of sensor fusion provides optimal state estimation that is not directly measurable. Given the observations, the states to be estimated are the linear acceleration, velocity and position of the vehicle. In order to reduce the computational complexity of the Kalman filter algorithm, the triaxial Kalman filter is decomposed into three single-axis Kalman filters, thereby reducing the computation load. According to (1), (2), (4), and (5), we define two discrete x axis vectors in the following (Barshan and Durrant-Whyte, 1995):

$$\begin{aligned} X(k) &= [x(k) \quad v_x(k) \quad a_x(k) \quad v(k) \quad a_{xm}(k) \quad a_{ym}(k) \quad a_{zm}(k)]^T, \\ Z(k) &= [z_v(k) \quad z_{axm}(k) \quad z_{aym}(k) \quad z_{azm}(k)]^T. \end{aligned}$$

Thus, a discrete X axis matrix state equation can be of the form

$$X(k+1) = F_x \cdot X(k) + G_x \cdot W_x(k), \quad (6)$$

where

$$F_x = \begin{bmatrix} 1 & \Delta t & 0 & 0 & 0 & 0 \\ 0 & 0 & \Delta t & \cos \theta(k) \cos \rho(k) & 0 & 0 \\ 0 & 0 & 0 & 0 & \cos \theta(k) \cos \rho(k) & 0 \\ 0 & 0 & 0 & 1 & 0 & 0 \\ 0 & 0 & 0 & 0 & 0 & 1 \\ 0 & 0 & 0 & 0 & 0 & 0 \\ 0 & 0 & 0 & 0 & 0 & 0 \\ & & 0 & 0 & 0 & 0 \\ & & 0 & 0 & 0 & 0 \\ & & -\sin \theta(k) \cos \rho(k) & -\sin \theta(k) \sin \rho(k) & 0 & 0 \\ & & 0 & 0 & 0 & 0 \\ & & 0 & 0 & 0 & 0 \\ & & 1 & 0 & 0 & 0 \\ & & 0 & 0 & 1 & 0 \end{bmatrix},$$

$$G_x = \begin{bmatrix} 0 & 0 & 0 & 0 \\ 0 & 0 & 0 & 0 \\ 0 & 0 & 0 & 0 \\ 1 & 0 & 0 & 0 \\ 0 & 1 & 0 & 0 \\ 0 & 0 & 1 & 0 \\ 0 & 0 & 0 & 1 \end{bmatrix}$$

and the measurement noise $W_x(k) = [\omega_v(k) \ \omega_{axm}(k) \ \omega_{aym}(k) \ \omega_{azm}(k)]^T$ is a white Gaussian distribution noise vector with zero-mean and covariance matrix given by $Q_x = \text{diag}\{q_v(k), q_{axm}(k), q_{aym}(k), q_{azm}(k)\}$, i.e., $W(k) \sim N(0, Q_x(k))$.

The discrete x axis matrix measurement equation is then expressed by

$$Z_x(k) = H_x \cdot X(k) + V_x(k), \quad (7)$$

where

$$H_x = \begin{bmatrix} 0 & 0 & 0 & 1 & 0 & 0 & 0 \\ 0 & 0 & 0 & 0 & 1 & 0 & 0 \\ 0 & 0 & 0 & 0 & 0 & 1 & 0 \\ 0 & 0 & 0 & 0 & 0 & 0 & 1 \end{bmatrix}$$

and the measurement noise $V_x = [v_v(k) \ v_{axm}(k) \ v_{aym}(k) \ v_{azm}(k)]^T$ is a zero-mean white Gaussian vector with the covariance of $R_x = \text{diag}\{\delta_v(k), \delta_{axm}(k), \delta_{aym}(k), \delta_{azm}(k)\}$, i.e., $V_x(k) \sim N(0, R_x(k))$.

A standard Kalman filter algorithm is utilized to obtain the optimal state estimates of the x -axis dynamics of the vehicle. Thus, the best x -axis position estimate of the vehicle can be obtained from $\hat{X}(k/k) = \hat{X}_x(k/k)$. Using the same method, we can obtain the best y -axis position estimate, $\hat{Y}(k/k) = \hat{X}_y(k/k)$, and the best z -axis position estimate, $\hat{Z}(k/k) = \hat{X}_z(k/k)$, respectively.

4. EKF-Based Sensor Fusion for Integrating INS and Ultrasonic Location System

The ultrasonic location subsystem will be employed to calibrate the posture information originally provided by the INS system. When the robot moves into the effective coverage area of ultrasonic signals, its posture can be updated using the ultrasonic TOF signals. An EKF-based sensor fusion algorithm for merging ultrasonic and INS measurements is proposed as follows:

Step 1. Using the previous INS algorithm, the position x , y , z and the orientation θ of the robot can be determined in the reference coordinate

$$\begin{bmatrix} x(k+1) \\ y(k+1) \\ z(k+1) \\ \theta(k+1) \end{bmatrix} = \begin{bmatrix} x(k) \\ y(k) \\ z(k) \\ \theta(k) \end{bmatrix} + \begin{bmatrix} \omega_x(k) \\ \omega_y(k) \\ \omega_z(k) \\ \omega_\theta(k) \end{bmatrix}, \quad (8)$$

where $\omega_x(k)$, $\omega_y(k)$ and $\omega_z(k)$ denote the errors of the INS position estimates, and $\omega_\theta(k)$ represents the orientation variations due to magnetic interference. Moreover, the process noises are assumed to be discrete-time, zero-mean white Gaussian sequences with diagonal covariance matrix $Q(k) = \text{diag}\{q_x(k), q_y(k), q_z(k), q_\theta(k)\}$.

Step 2. Assume that the robot moves slowly; his four TOF measurements of the ultrasonic localization system are expressed using the following matrix equation

$$\begin{bmatrix} t_1(k) - t_{d1} \\ t_2(k) - t_{d2} \\ t_3(k) - t_{d3} \\ t_4(k) - t_{d4} \end{bmatrix} = \begin{bmatrix} D_1/c \\ D_2/c \\ D_3/c \\ D_4/c \end{bmatrix} + \begin{bmatrix} n_1(k) \\ n_2(k) \\ n_3(k) \\ n_4(k) \end{bmatrix}, \quad (9)$$

where

$$D_1 = \sqrt{(x_1 - x_5)^2 + (y_1 - y_5)^2 + (z_1 - z_5)^2},$$

$$D_2 = \sqrt{(x_2 - x_5)^2 + (y_2 - y_5)^2 + (z_2 - z_5)^2},$$

$$D_3 = \sqrt{(x_3 - x_5)^2 + (y_3 - y_5)^2 + (z_3 - z_5)^2},$$

$$D_4 = \sqrt{(x_4 - x_5)^2 + (y_4 - y_5)^2 + (z_4 - z_5)^2}.$$

In (9), t_i and t_{di} denote the TOF and the time delay of the i th receiver, respectively. Measurement noises $n_1(k)$, $n_2(k)$, $n_3(k)$ and $n_4(k)$ are regarded as mutually independent, zero-mean white Gaussian processes with covariance $R(k) = \text{diag}\{\delta_1(k), \delta_2(k), \delta_3(k), \delta_4(k)\}$.

Equations (8) and (9) can be more compactly rewritten in the vector-matrix form:

$$X(k+1) = X(k) + W(k), \quad (10)$$

$$Z(k) = h(X(k)) + V(k), \quad (11)$$

where

$$X(k) = [x(k) \quad y(k) \quad z(k) \quad \theta(k)]^T,$$

$$Z(k) = [t_1(k) - t_{d1} \quad t_2(k) - t_{d2} \quad t_3(k) - t_{d3} \quad t_4(k) - t_{d4}]^T,$$

$$W(k) = [\omega_x(k) \quad \omega_y(k) \quad \omega_z(k) \quad \omega_\theta(k)]^T,$$

$$V(k) = [n_1(k) \quad n_2(k) \quad n_3(k) \quad n_4(k)]^T,$$

$$h(X(k)) = \begin{bmatrix} D_1/c & D_2/c & D_3/c & D_4/c \end{bmatrix}^T.$$

Step 3. Apply the standard EKF algorithm in (Saridis, 1995) to find the best estimate of $X(k)$. Notice that applying the standard EKF algorithm requires that the Jacobian matrix H of $Z(k)$ is given by

$$H \begin{pmatrix} x \\ y \\ z \\ \theta \end{pmatrix} = \begin{bmatrix} \frac{x_1 - x_5}{cD_1} & \frac{y_1 - y_5}{cD_1} & \frac{z_1 - z_5}{cD_1} & \frac{A_1}{c^2} \\ \frac{x_2 - x_5}{cD_2} & \frac{y_2 - y_5}{cD_2} & \frac{z_2 - z_5}{cD_2} & \frac{A_2}{c^2} \\ \frac{x_3 - x_5}{cD_3} & \frac{y_3 - y_5}{cD_3} & \frac{z_3 - z_5}{cD_3} & \frac{A_3}{c^2} \\ \frac{x_4 - x_5}{cD_4} & \frac{y_4 - y_5}{cD_4} & \frac{z_4 - z_5}{cD_4} & 0 \end{bmatrix},$$

where

$$\begin{aligned} A_1 &= \left[x - 0.5 \cdot d \cos \theta - \frac{\sqrt{3}}{2} d \sin \theta - x_5 \right] \cdot \left[0.5 \cdot d \sin \theta - \frac{\sqrt{3}}{2} d \cos \theta \right] \\ &\quad + \left[y + \frac{\sqrt{3}}{2} \cos \theta - 0.5 \cdot d \sin \theta - y_5 \right] \cdot \left[-\frac{\sqrt{3}}{2} \sin \theta - 0.5 \cdot d \sin \theta \right], \\ A_2 &= \left[x - 0.5 \cdot d \cos \theta + \frac{\sqrt{3}}{2} d \sin \theta - x_5 \right] \cdot \left[0.5 \cdot d \sin \theta + \frac{\sqrt{3}}{2} d \cos \theta \right] \\ &\quad + \left[y - \frac{\sqrt{3}}{2} \cos \theta - 0.5 \cdot d \sin \theta - y_5 \right] \cdot \left[\frac{\sqrt{3}}{2} \sin \theta - 0.5 \cdot d \cos \theta \right], \\ A_3 &= [x + d \cos \theta - x_5] \cdot [-d \sin \theta] + [y + d \sin \theta - y_5] \cdot [d \cos \theta]. \end{aligned}$$

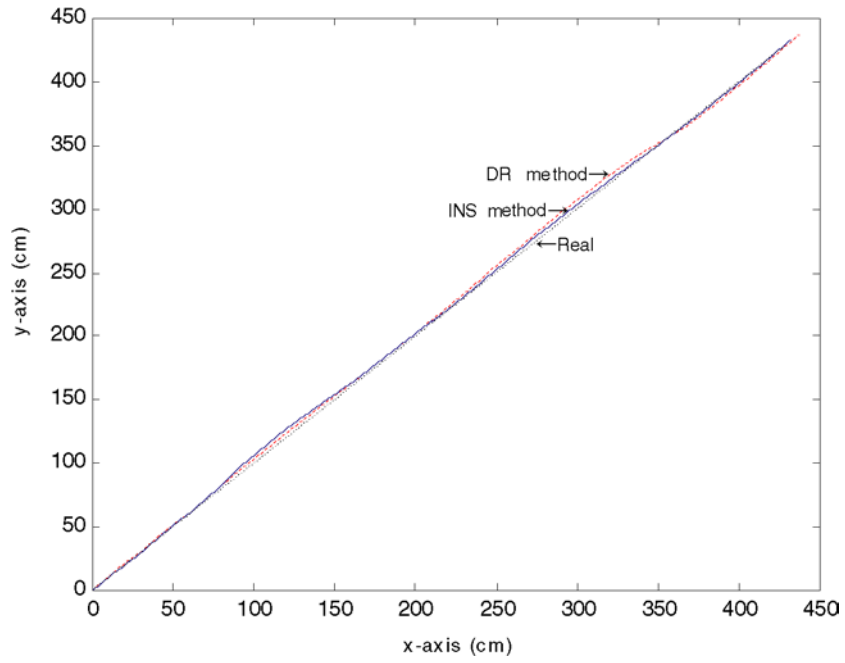
With a good initialization of $\hat{X}(0/0)$ and $\tilde{P}(0/0)$, the EKF-based sensor fusion algorithm will yield a good estimate of the vehicle posture.

5. Experimental Results and Discussion

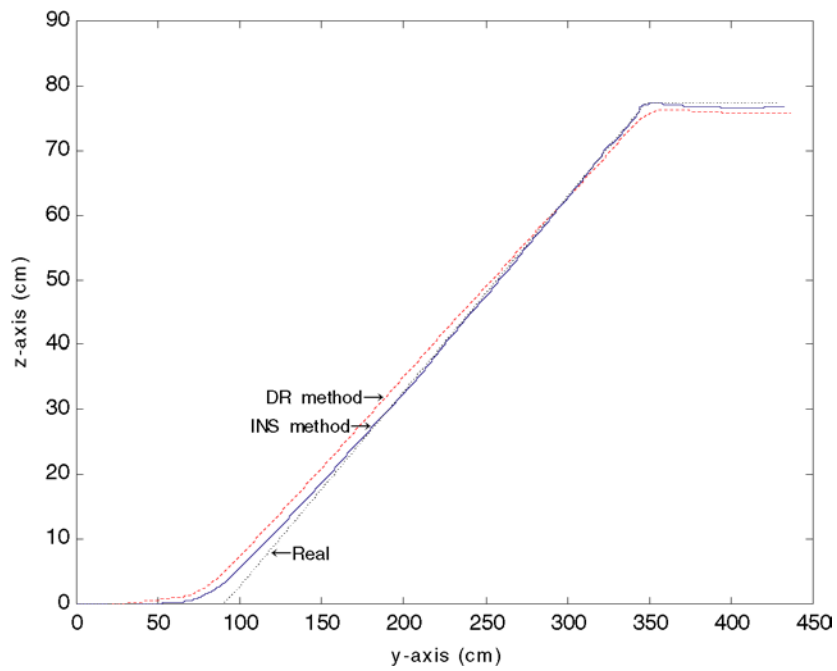
Two experiments were conducted in this section to investigate the feasibility, accuracy and performance of the proposed method: one is for the stand-alone INS system; the other is for dynamic properties of the integrated INS/Ultrasonic system.

5.1. INS PERFORMANCE EVALUATION

The aim of the experiment of the stand-alone INS system on two different terrains: an inclined terrain and an irregular terrain, is to study what accuracy and precision the experimental INS system achieves. Before proceeding with the experiment, all important components, such as the speedometer and the triaxial accelerometer, were correctly calibrated, hereby allowing us to compute the statistical parameters of their noise model: $q_v = \delta_v = 0.21 \text{ cm/sec}^2$, $q_{axm} = \delta_{axm} = 22.57 \text{ cm/sec}^2$,



(a)



(b)

Figure 6. (a) x - y trajectories of the robot over inclined terrain; (b) y - z trajectories of the robot over inclined terrain.

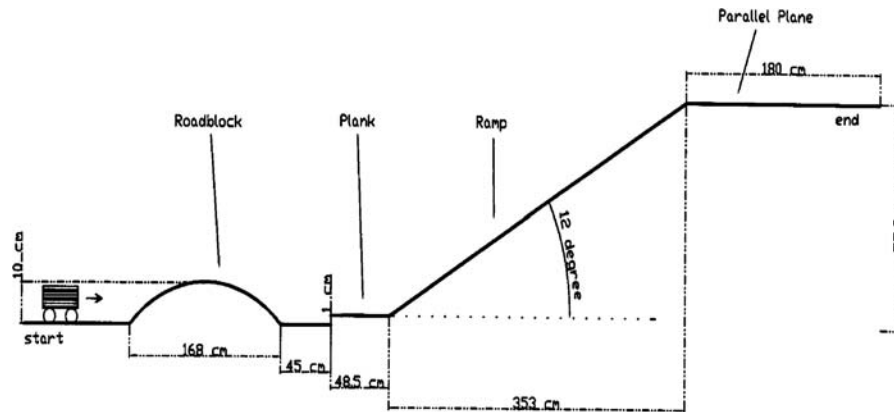


Figure 7. Schematics of the irregular terrain.

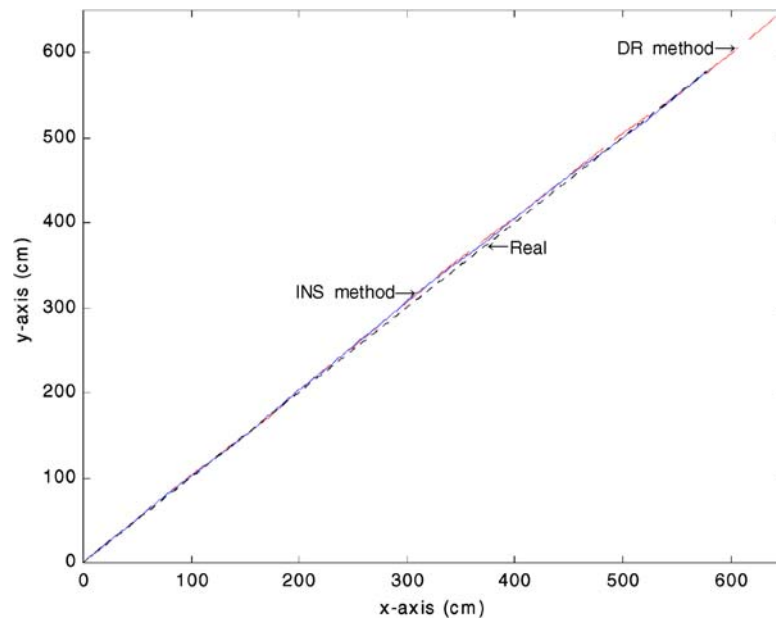
$q_{aym} = \delta_{aym} = 22.84 \text{ cm/sec}^2$ and $q_{azm} = \delta_{azm} = 22.18 \text{ cm/sec}^2$. In the experiments, the robot was assumed to move in a line with fixed heading angle of 45° .

To accomplish the inclined terrain experiment, a path profile with the dimension $366 \text{ (D)} \cdot 90 \text{ (W)} \cdot 77.3 \text{ (H)} \text{ cm}$ and the pitch angle of 12° and with a parallel plane (180 cm in length) at the top of the ramp is made in (Lai, 2000). The robot was controlled to move straight up to the inclined terrain with the fixed heading angle of 45° . Figure 6 shows the experimental data. The result in Figure 6 indicates that the proposed INS system performs as well as 3D DR method. To compare the INS system with the DR system in detail, a complicated terrain environment is constructed to examine the feasibility, and accuracy of the INS system. Figure 7 depicts the experimental terrain with a steep gradient and undulating profile. Similarly, to make the experiment simple and easy, let the robot move up the inclined terrain with the fixed heading angle of 45° . Figure 8 displays the results of this experiment where the true final position was at the localization (577.85 cm, 577.85 cm, 77.38 cm). The final position estimated by the INS system was (592.23 cm, 592.06 cm, 75.90 cm) and the DR system gives it at (641.81 cm, 641.70 cm, 83.71 cm). The experimental results reveal that for the uneven terrain, the INS system outperforms the 3D DR system even over such a short distance; moreover, the INS system circumvents the unsolved problem of wheel slippage.

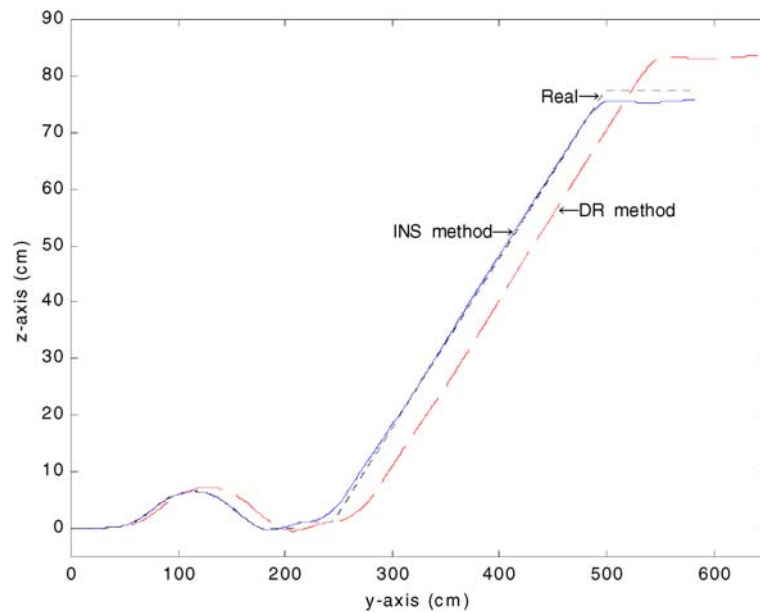
5.2. INS/ULTRASONIC EXPERIMENTAL RESULTS AND DISCUSSION

The experiment of the INS/Ultrasonic system focuses on exploring how the system overcomes the accumulation error problem caused by the proposed INS system while the robot travels over uneven terrain. As in the previous experiment, the statistical parameters of the proposed INS system output must be correctly computed, thus obtaining $q_x = 0.74 \text{ cm}$, $q_y = 0.76 \text{ cm}$, $q_z = 0.77 \text{ cm}$ and $q_\theta = 2^\circ$.

The ultrasonic transmitter was located at the perspecified position (167.6 cm, 237.0 cm, 252.0 cm) with respect to the world frame. While the experiment was

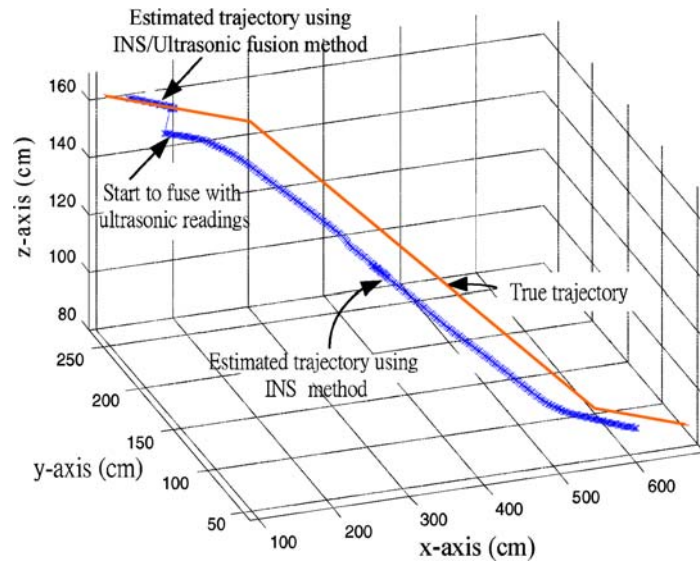


(a)

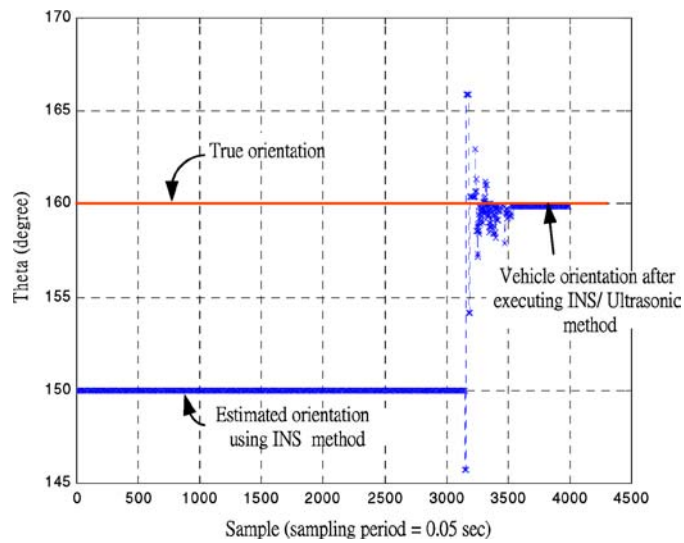


(b)

Figure 8. (a) x - y trajectories of the robot over the irregular terrain; (b) y - z trajectories of the robot over the irregular terrain.



(a)



(b)

Figure 9. (a) 3D trajectory of the robot over the irregular terrain (move up cases); (b) time history of the robot heading estimate.

being performed, the mean ambient temperature was fixed to be almost constant ($T = 22.3^{\circ}\text{C}$) with small temperature fluctuations allowed ($\Delta T = \pm 0.3^{\circ}\text{C}$). Therefore the correct speed of the ultrasonic sound was 34456.88 cm/sec . Thus, the standard deviations of the TOF measurements were computed as $\sigma_1 = 4.2 \mu\text{s}$, $\sigma_2 = 4.5 \mu\text{s}$, $\sigma_3 = 4.4 \mu\text{s}$ and $\sigma_4 = 4.3 \mu\text{s}$. The time delays of the ultrasonic

transmitter/receiver modules were measured as $t_{d1} = 0.452$ ms, $t_{d2} = 0.455$ ms, $t_{d3} = 0.454$ ms and $t_{d4} = 0.432$ ms. In addition, other parameters were measured and given by spaced distance $d = 15$ cm and the sampling period $T_s = 0.05$ sec.

To make the experiment successful, the vehicle was steered to move up along a straight line with an erroneous heading angle of 150° over the previous inclined terrain. Figure 9 shows the resultant outcomes. When mobile vehicle reached the area which was covered by the ultrasonic wave, we used the ultrasonic localization system together with the proposed EKF algorithm to correct the posture estimate. The actual final posture was located at (126.0 cm, 252.0 cm, 164.3 cm, 160°), while the final position and orientation estimated by the integrated INS/Ultrasonic system were (125.0 cm, 251.82 cm, 164.87 cm, 159.847°). One more experiment was conducted to provide sufficient information to verify the efficacy of the proposed method. The vehicle was steered to move down along a straight line with an erroneous heading angle of 180° over the previous inclined terrain. Figure 10 shows the results; the results are very similar to the previous ones, and these results provide additional evidences to justify the effectiveness of the proposed method. The experimental results in Figures 9 and 10 indicate that the INS/Ultrasonic system gives a better estimate of the vehicle posture.

6. Conclusions

This paper has incorporated the INS and ultrasonic sensor integration system for finding a better current posture of a mobile robot traveling over uneven terrain. The integrated system combines the strong points of the two subsystems for yielding better position accuracy but less computation requirement. The proposed INS system has been shown capable of providing low-cost, high-precision posture information for the vehicle traveling over short distances. The initial covariance of the Kalman filter has a tremendous effect on the performance of the navigation system and can be adjusted based on the system process noise and limitations of the sensors. By choosing process covariance matrix $Q(k)$ and noise covariance matrix $R(k)$ appropriately, the effects of process uncertainties and sensor inaccuracies can be minimized by the Kalman filtering process. Through the experimental results over the uneven terrain, the INS/Ultrasonic system has been proven capable of having position accuracy of less than 1 cm and orientation accuracy of less than 1° . An important topic for future research might be to address the initialization problem of the robot using ultrasonics.

Acknowledgement

The authors gratefully acknowledge financial support from the National Science Council of the Republic of China under Grant NSC 91-2213-E-005-002.

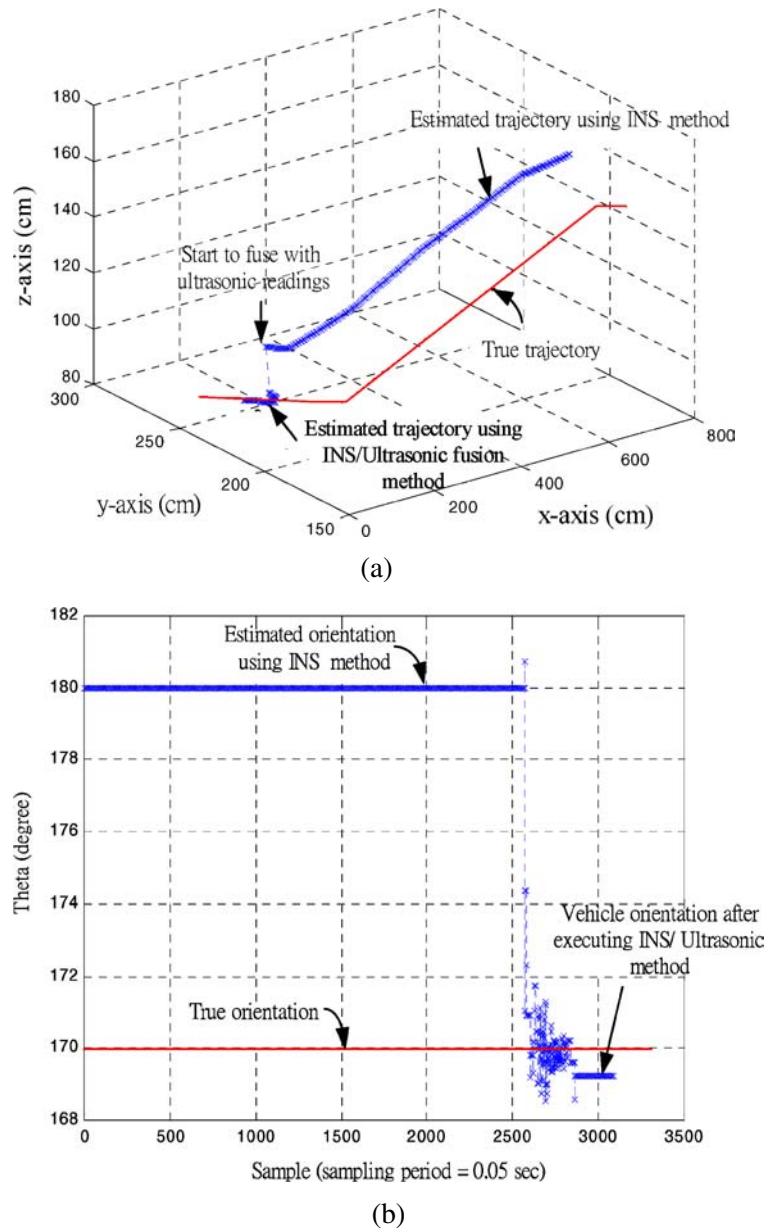


Figure 10. (a) 3D trajectory of the robot over the irregular terrain (move down cases); (b) time history of the robot heading estimate.

References

- Barshan, B. and Durrant-Whyte, H. F.: 1994, Orientation estimate for mobile robots using gyroscopic information, in: *Internat. Conf. on Intelligent Robots and Systems*, Munich, Germany, pp. 2243–2248.

- Barshan, B. and Durrant-Whyte, H. F.: 1995, Inertial navigation systems mobile robots, *IEEE Trans. Robotics Automat.* **2**(3), 328–342.
- Borenstein, J., Everett, H. R., and Feng, L.: 1996, *Navigating Mobile Robots: Systems and Techniques*, AK Peters.
- Drumheller, M.: 1987, Mobile robot location using sonar, *IEEE Trans. Pattern Anal. Mach. Intelligence* **9**, 325–332.
- Figueroa, F. and Mahajan, A.: 1994, A robust navigation system for autonomous vehicles using ultrasonics, *Control Engrg. Practice* **2**(1), 49–59.
- Foxlin, E. M.: 2002, Generalized architecture for simultaneous localization, auto-calibration, and map-building, in: *IEEE/RSJ Internat. Conf. on Intelligent Robots and Systems*, Vol. 1, pp. 527–533.
- Fujisawa, S., Yamamoto, T., Suita, Y., Ryuman, N., Sogo, H., and Yoshida, T.: 2001, Development of path tracking control for omni-directional mobile robot using visual servo system, in: *27th Annual Conf. of the IEEE*, Vol. 3, Industrial Electronics Society, IECON, pp. 2166–2170.
- Kim, J., Jee, G. I., Lee, J. G., and Sung, T.-K.: 1995, Calibration of DR and GPS/DR integration, in: *Proc. of the 2nd ITS World Congress*, Vol. 2, pp. 547–552.
- Lai, S. W.: 2000, Multisensorial self-localization of an autonomous mobile robot over uneven terrain, MS Thesis, Department of Electrical Engineering, National Chung-Hsing University.
- Leonard, J. J. and Durrant-Whyte, H. F.: 1992, *Directed Sonar Sensing for Mobile Robot Navigation*, Kluwer, Dordrecht.
- Mae, Y., Masuda, T., Arai, T., and Inoue, K.: 2001, Error analysis of dead reckoning of multi-legged robots, in: *Proc. of IEEE/RSJ Internat. Conf. on Intelligent Robots and Systems*, Vol. 3, pp. 1558–1563.
- Maksarov, D. and Durrant-Whyte, H.: 1995, Mobile vehicle navigation in unknown environments: A multiple hypothesis approach, *IEEE Proc. Control Appl. Theory* **142**(4), 385–400.
- Maybeck, P. S.: 1979, *Stochastic Models, Estimation, and Control*, Vol. 1, Academic Press, New York.
- Sabatini, M.: 1995, A digital signal processing techniques for compensating ultrasonic sensors, *IEEE Trans. Instrument Measm.* **44**(4), 869–874.
- Saridis, G. N.: 1995, *Stochastic Processes, Estimation, and Control: The Entropy Approach*, Wiley, New York.
- Song, K. T. and Suen, Y. H.: 1996, Design and implementation of a path tracking controller with the capacity of obstacle avoidance, in: *Proc. of 1996 Automatic Control Conf.*, Taipei, Taiwan, pp. 134–139.
- Sorenson, H. W.: 1990, *Kalman Filtering Theory and Application*, IEEE Press, New York.
- Triggs, B.: 1994, Model-based sonar localization for mobile robots, *Robotics Automom. Systems* **12**, 173–186.
- Tsai, C. C.: 1998, A localization system of a mobile robot by fusing dead-reckoning and ultrasonic measurements, *IEEE Trans. Industrial Measm.* **47**(5), 1399–1404.
- Tsai, C. C., Lai, S. W., and Lin, H. H.: 2003, Multisensorial 3D posture determination of a mobile robot using inertial and ultrasonic sensors, in: *CD-ROM Proc. of Internat. Conf. on Automation Technology*, Chia-Yi, Taiwan, R. O. C., F126.
- Vaganay, J., Aldon, M. J., and Poimnier, A.: 1993, Mobile robot attitude estimation by fusion of inertial data, in: *Proc. of IEEE Internat. Conf. on Robotics and Automation*, Atlanta, GA, pp. 3243–3248.
- Wang, J. P., Tian, W. F., and Jin, Z. H.: 2003, Study on integrated micro inertial navigation system/GPS for land vehicles, in: *Intelligent Transportation Systems, Proc. of IEEE*, Vol. 2, pp. 1650–1653.